A STUDY OF THE QUALITY OF CARROT ROOT CLEANING WITH A SPIRAL CLEANER: SOIL SEPARATION AND MECHANICAL DAMAGE
/
ДОСЛІДЖЕННЯ ЯКОСТІ ОЧИЩЕННЯ КОРЕНЕПЛОДІВ МОРКВИ СПІРАЛЬНИМ ОЧИСНИКОМ: ВІДОКРЕМЛЕННЯ ҐРУНТУ ТА МЕХАНІЧНІ ПОШКОДЖЕННЯ

Volodymyr BULGAKOV[1)], **Oleksandr MATSUIEV**[2,*)], **Lucretia POPA**[3)], **Jüri OLT**[4)]
[1)] National University of Life and Environmental Sciences of Ukraine, Kyiv, Ukraine
[2)] Institute of Mechanics and Automation of Agroindustrial Production of the National Academy of Agrarian Sciences of Ukraine, Hlevakha, Ukraine
[3)] Research Institute for Agriculture Economy and Rural Development – ICEADR Bucharest, Romania
[4)] Estonian University of Life Sciences, Institute of Forestry and Engineering, Chair of Biosystems Engineering, Tartu, Estonia
**Corresponding author: Oleksandr Matsuiev; e-mail: oleksandr.matsuiev@claas.com; ORCID: 0009-0000-9878-0591*
DOI: https://doi.org/10.35633/inmateh-79-98

Keywords: *carrot roots; spiral cleaner; soil separation; mechanical damage; angular velocity; entry orientation.*

ABSTRACT
This study combined two complementary criteria for evaluating a spiral cleaner for carrot roots: the spatial distribution of separated soil and the occurrence of mechanical damage. A laboratory test rig with a V-shaped cleaning trough formed by cantilevered spiral springs and driven brushes equipped with elastic rods was used. Nantes carrot roots were tested at cleaner-shaft angular velocities of 27.2, 31.4, and 35.6 rad·s⁻¹ and in two entry orientations: tail-end-first and thicker-end-first. Separated soil was collected in three consecutive zones along the transport path. Mechanical damage was assessed immediately after cleaning and again after 24 h using samples of 100 roots. Zone I accounted for 38–48% of the separated soil, Zone II for 33–41%, and Zone III for 11–28%. Increasing the angular velocity shifted soil separation toward the inlet section. The proportion of undamaged roots decreased from 66% to 44% for the tail-end-first orientation and from 75% to 59% for the thicker-end-first orientation. The thicker-end-first orientation resulted in 9–15 percentage points more undamaged roots and reduced the combined proportion of cracks, broken tail ends, and impact bruises from 13–25% to 5–14%. Under the tested conditions, an angular velocity of 27.2 rad·s⁻¹ with the thicker-end-first orientation was identified as the preferred low-damage operating condition. The results provide a basis for further multifactor optimization incorporating residual adhering soil, throughput, and energy consumption as additional evaluation criteria.

РЕЗЮМЕ
У дослідженні поєднано два взаємодоповнювальні критерії оцінювання спірального очисника коренеплодів моркви: просторовий розподіл відокремленого ґрунту та виникнення механічних пошкоджень. Використано лабораторну установку з V-подібним очисним руслом, утвореним консольними спіральними пружинами і приводними щітками з еластичними прутками. Коренеплоди моркви сорту «Нантська» досліджували за кутових швидкостей обертання валів 27,2; 31,4 і 35,6 рад·с⁻¹ та двох орієнтацій подавання: хвостовою або товстішою частиною вперед. Відокремлений ґрунт збирали у трьох послідовних зонах за довжиною транспортування. Механічні пошкодження оцінювали безпосередньо після очищення та повторно через 24 год у вибірках по 100 коренеплодів. У зоні I відокремлювалося 38-48% ґрунту, у зоні II – 33-41%, у зоні III – 11-28%. Зі збільшенням кутової швидкості процес зміщувався до початкової ділянки русла. Частка непошкоджених коренеплодів зменшилася з 66 до 44% за руху хвостовою частиною вперед і з 75 до 59% за руху товстішою частиною вперед. Друга орієнтація забезпечила на 9-15 відсоткових пунктів більше непошкоджених коренеплодів та зменшила сумарну частку тріщин, обламаних хвостових частин і плям від удару з 13-25 до 5-14%. За досліджених умов переважним малотравматичним режимом визначено режим, що відповідає 27,2 рад·с⁻¹ за подавання коренеплодів моркви товстішою частиною вперед.

INTRODUCTION
Cleaning the carrot-root heap after digging must simultaneously remove soil impurities and plant residues while preserving the marketable integrity of the produce. This task is complicated by the elongated shape of the roots, the small local contact area with the working elements, and differences in mechanical strength between the crown and tail sections.

Data on the geometric and mechanical properties of carrots indicate that impacts, local compression and bending may cause skin abrasions, cracks, internal bruising and tail-end breakage (*Jahanbakhshi et al., 2018; Nath et al., 2019; Stopa et al., 2017; Stopa et al., 2019; Xia et al., 2021*). Such damage impairs storability and reduces the proportion of marketable roots.

Modern carrot harvesters use digging shares, clamping-and-conveying belts, topping devices and cleaning units. Studies of these assemblies show that performance depends strongly on operating speed, working-element geometry and root orientation during interaction (*Jin et al., 2016; Jin et al., 2020; Rybacki et al., 2024; Wang et al., 2025a; Wang et al., 2025b; Yasmeen et al., 2023; Zeng et al., 2018; Zhao et al., 2024*). Machine-vision systems are also being developed for rapid defect detection; however, they do not eliminate the need for a mechanically gentle process (*Zhou et al., 2023*).

Spiral working elements are promising for separating heaps of root and tuber crops because they combine conveying, screening of fine impurities and self-cleaning from adhering moist soil. Scientific principles developed for potatoes and other root crops confirm that angular velocity, spiral geometry and the interaction scheme affect separation intensity and product damage (*Bulgakov et al., 2017; Bulgakov et al., 2018; Guo and Campanella, 2017; Hevko et al., 2020; Hoffmann et al., 2018; Issa et al., 2020*). However, direct transfer of such operating modes to carrots is inappropriate because of their elongated shape and the greater vulnerability of the tail end.

Recent studies on optimized conveying and separation systems for *Panax notoginseng* and potato have combined bench or field experiments with coupled simulation, while whole-machine studies on *Panax notoginseng* and white radish have emphasized the importance of controlling crop damage (*Chen et al., 2024; Pan et al., 2025; Wang et al., 2023; Xiao et al., 2023; Zhang et al., 2016*). These results provide useful quantitative benchmarks, but their operating modes and quality indices are not directly transferable to a dedicated carrot cleaner because carrot roots are elongated, orientation-sensitive and readily bruised.

In previous studies, soil separation and carrot damage were considered separately, preventing an integrated assessment of the technological trade-off between cleaning intensity and root preservation. The objective of this study was to determine the effects of spiral-cleaner shaft angular velocity and carrot-root entry orientation on the distribution of separated soil along the cleaning trough and on the pattern of mechanical damage, and to identify the preferred low-damage operating mode within the investigated factor range.

MATERIALS AND METHODS

Experimental studies were conducted using a laboratory spiral-cleaner test rig (Fig. 1). An intermediate frame 3 was attached to the main frame *1* by a hinge *2*; its inclination was adjusted by a screw mechanism *4* with a guide *5* and actuator *6*. A working-unit frame *8* was mounted on elastic supports *7*. Each spiral working element comprised a drum *9*, a cylindrical spring *10*, a shaft *11* and a bearing assembly *12*. The free end of each spiral rested, through bracket *13*, on a movable support *15* connected to vibrator *16*. Spiral springs *10* and driven cleaning brushes *14* formed a V-shaped cleaning trough.

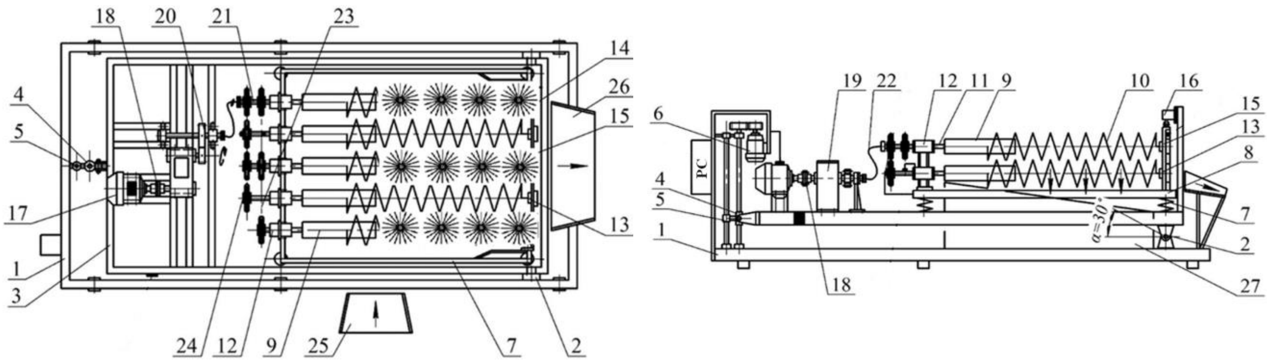

a) b)

Fig. 1 – Schematic of the laboratory test rig:
a – top view; b – side view

1 - main frame; 2 - hinge; 3 - intermediate frame; 4 - screw mechanism; 5 - guide; 6 - actuator; 7 - elastic supports; 8 - working-unit frame; 9 - drum; 10 - cylindrical spring; 11 - shaft; 12 - bearing housing; 13 - bracket; 14 - cleaning brushes; 15 - movable support; 16 - vibrator; 17 - electric motor; 18 - coupling; 19 - continuously variable transmission; 20 - spur gear transmission; 21 - drive shaft; 22 - flexible shaft; 23, 24 - chain drives; 25 - feed chute; 26 - discharge chute; 27 - soil collection tray

The bottom and one side surface of the trough were formed by cantilevered spiral springs whose turns conveyed the material from the inlet towards the outlet. The opposite side surface was formed by flat driven brushes with elastic rods. Rotation of the spirals provided axial conveying and allowed soil to pass through the inter-turn gaps, while the brushes assisted root movement and removal of fine impurities. The mutual overlap of adjacent spirals promoted self-cleaning. General views of the test rig, working elements, cleaning trough and soil-collection zones are shown in Fig. 2.

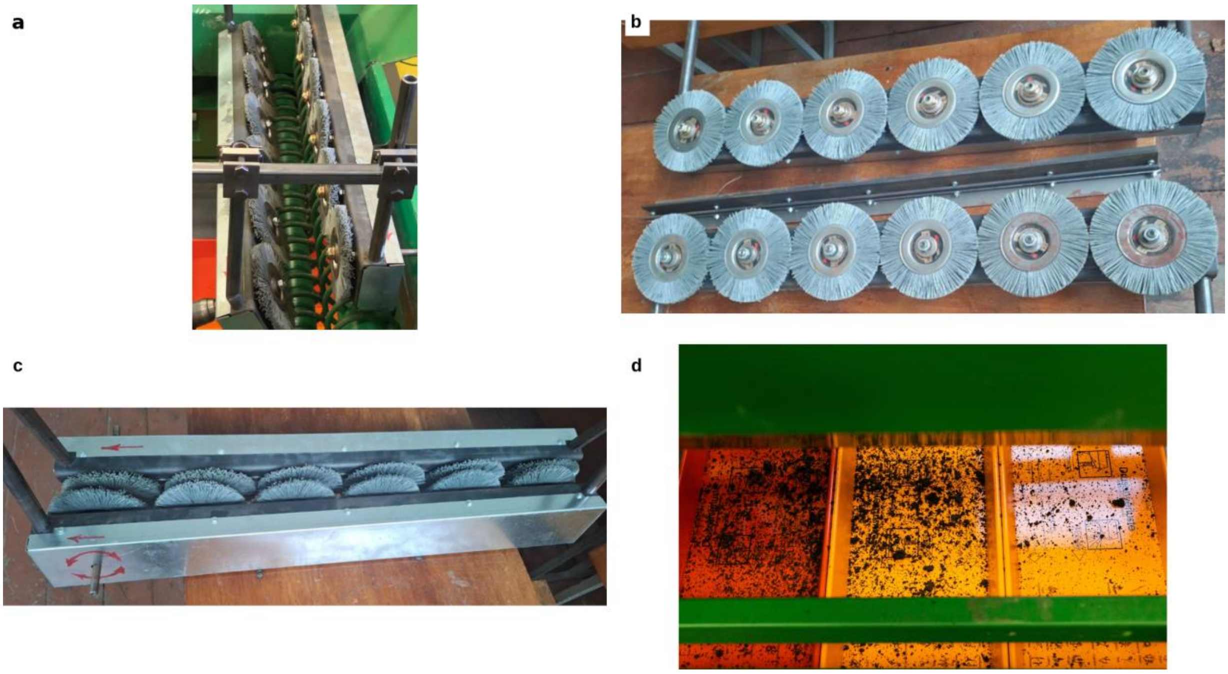

Fig. 2 – Components of the experimental test rig:
a – general view; b – frames with driven brushes; c – cleaning trough; d – trays for collecting soil by zone

Pre-dug roots of the Nantes carrot cultivar, predominantly elongated-cylindrical in shape, were used in the experiments. No cleaning elements were used during digging. Roots without initial mechanical damage were selected, transported separately and weighed on an electronic balance with 0.1 g resolution. The permissible mass deviation within each experimental group was ±5 g. For damage assessment, all adhering soil was removed from the roots beforehand so that surface defects would not be obscured.

Table 1

Factors and experimental conditions

Parameter or indicator	Levels / assessment procedure	Unit / note
Shaft angular velocity, ω	27.2; 31.4; 35.6	$rad \cdot s^{-1}$
Entry orientation A	tail-end-first	–
Entry orientation B	thicker-end-first	–
Number of replicate soil-separation test series	3	for each operating mode
Damage-assessment sample size	100	roots per operating mode (600 total)
Assessment of latent impact damage	repeat inspection after 24	h

Experimental design and scope. Two complementary experimental series were performed for each of the six operating modes: (i) zonal collection of soil released from roots carrying adhering soil and (ii) mechanical-damage assessment using roots from which adhering soil had been removed before testing. The soil-separation series comprised three replicate test runs per mode with group masses matched to within ±5 g. The damage distribution was determined from 100 roots per mode (600 roots in total).

Along the transport direction, the cleaning trough was conventionally divided into three consecutive sections. Zone I represented the initial impact-separation interaction, Zone II the steady-state cleaning stage, and Zone III the completion of cleaning before discharge. Soil passing through the working surface was collected in three separate trays. The share attributed to each zone was calculated as the mass of soil in the corresponding tray divided by the total mass collected in all three trays and was expressed as a percentage.

After passing through the cleaning trough, each root was inspected in two stages. Immediately after the test, skin abrasions, scratches, cracks and tail-end breakage were recorded. A second inspection was performed after 24 h to detect darkened bruises resulting from impact or severe local compression. The dimensions of damaged areas were measured with a vernier caliper. For each operating mode, the percentage distribution among six categories was calculated: 1 – no damage; 2 – skin abrasions; 3 – scratches; 4 – cracks; 5 – broken tail end; 6 – impact bruise.

Statistical analysis. The primary damage endpoint was the proportion of undamaged roots. A secondary endpoint, termed severe damage, combined cracks, broken tail ends and impact bruises. Wilson 95% confidence intervals were calculated for both endpoints. The effect of entry orientation across the three angular-velocity strata was assessed with the Cochran-Mantel-Haenszel test, and ordered trends across angular velocity were tested with the Cochran-Armitage trend test. All tests were two-sided with $\alpha = 0.05$. Because the available zonal soil data consisted of mode-level shares that sum to 100%, the soil-separation distribution was analyzed descriptively; no ANOVA or claim of a global optimum was made.

RESULTS

Under all operating modes, the largest proportion of separated soil was collected at the beginning of the cleaning trough. In the tail-end-first orientation, Zone I accounted for 42, 44 and 48% of the separated soil at ω = 27.2, 31.4 and 35.6 rad·s^{-1}, respectively. The share in Zone III decreased from 25 to 11%. In the thicker-end-first orientation, the share in Zone I was 38-45%, whereas that in Zone III was 17-28% (Fig. 3).

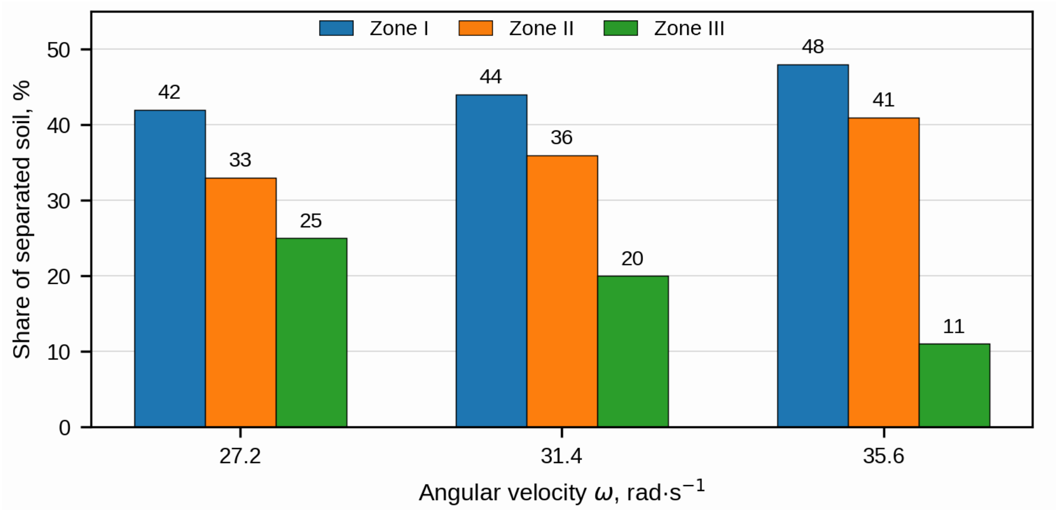

a)

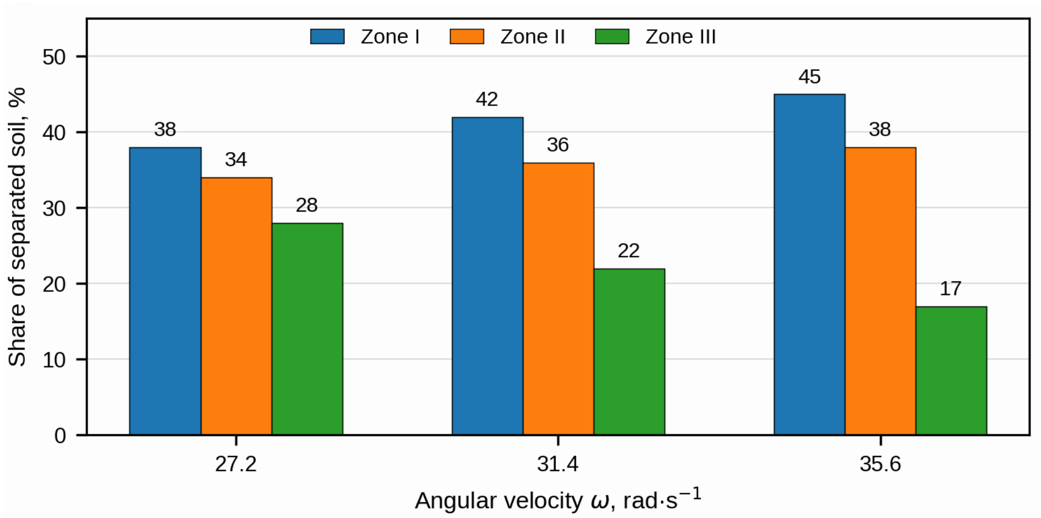

b)

Fig. 3 – Distribution of separated soil along the cleaning trough:
a – tail-end-first orientation; b – thicker-end-first orientation

Increasing angular velocity shifted the separation process towards Zone I in both entry orientations: its share increased by 6-7 percentage points, whereas the share in Zone III decreased by 11-14 percentage points. This indicated intensification of the initial interaction between the roots, spirals and brushes. With thicker-end-first feeding, the distribution along the trough was slightly more uniform: the Zone I share was 2-4 percentage points lower and the Zone III share 2-6 percentage points higher than with tail-end-first feeding.

Mechanical damage. Five types of defect were recorded: skin abrasions, scratches, cracks, broken tail ends and impact bruises, the last of which became clearly visible after 24 h (Fig. 4). The delayed appearance of impact bruises confirmed the need for two-stage inspection, because a single inspection immediately after cleaning would have underestimated the proportion of damaged roots. The delayed appearance of impact bruises confirmed the need for a two-stage inspection, as inspection conducted only immediately after cleaning would have underestimated the proportion of damaged roots.

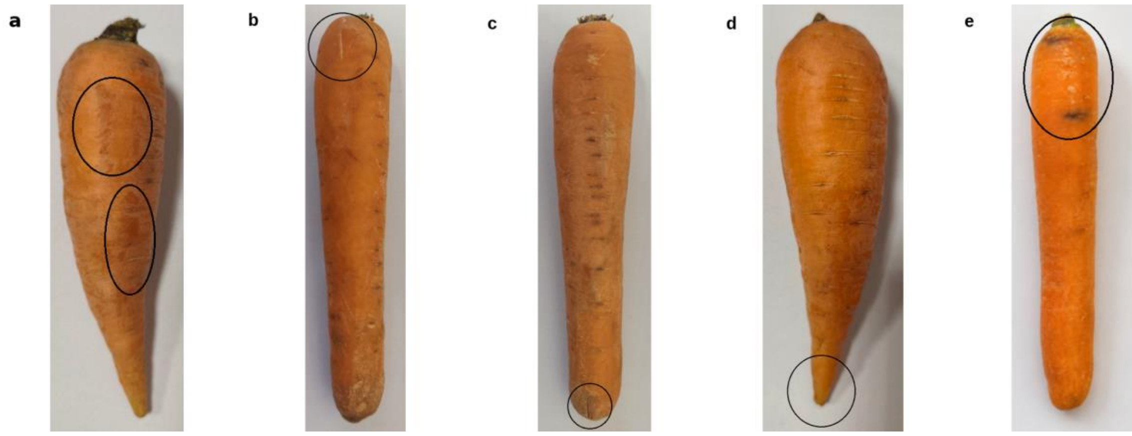

Fig. 4 – Types of mechanical damage to carrot roots:
a – skin abrasion; b – scratch; c – crack; d – broken tail end; e – impact bruise

In the tail-end-first orientation, the proportion of undamaged roots decreased from 66% at 27.2 rad·s^{-1} to 56% at 31.4 rad·s^{-1} and 44% at 35.6 rad·s^{-1}. All damage categories increased simultaneously: skin abrasions from 11 to 16%, scratches from 10 to 15%, cracks from 5 to 10%, broken tail ends from 5 to 8%, and impact bruises from 3 to 7% (Fig. 5a). Thus, increasing angular velocity intensified both superficial and structural defects.

In the thicker-end-first orientation, 75, 68 and 59% of roots remained undamaged at the three angular velocities, respectively (Fig. 5b). These values were 9, 12 and 15 percentage points higher than for the opposite orientation. The difference was particularly pronounced for more severe damage. The combined proportions of cracks, broken tail ends and impact bruises in the tail-end-first orientation were 13, 18 and 25%, compared with 5, 8 and 14% in the thicker-end-first orientation. Thus, the advantage of the thicker-end-first orientation increased with angular velocity.

Table 2

Statistical summary of mechanical-damage endpoints (n = 100 roots per operating mode)

Entry orientation	Angular velocity, ω, rad·s^{-1}	Undamaged roots, % (95% CI)	Severe damage, % (95% CI)
tail-end-first	27.2	66 (56.3-74.5)	13 (7.8-21.0)
tail-end-first	31.4	56 (46.2-65.3)	18 (11.7-26.7)
tail-end-first	35.6	44 (34.7-53.8)	25 (17.5-34.3)
thicker-end-first	27.2	75 (65.7-82.5)	5 (2.2-11.2)
thicker-end-first	31.4	68 (58.3-76.3)	8 (4.1-15.0)
thicker-end-first	35.6	59 (49.2-68.1)	14 (8.5-22.1)

Note: severe damage = cracks + broken tail ends + impact bruises; confidence intervals are Wilson intervals.

Across angular-velocity strata, thicker-end-first feeding increased the odds that a root remained undamaged (common OR = 1.69, 95% CI 1.20-2.36; $p = 0.002$) and reduced the odds of severe damage (common OR = 0.42, 95% CI 0.26-0.70; $p < 0.001$). The proportion of undamaged roots decreased significantly with angular velocity for both tail-end-first ($p = 0.002$) and thicker-end-first ($p = 0.016$) feeding, whereas severe damage increased ($p = 0.029$ and $p = 0.026$, respectively).

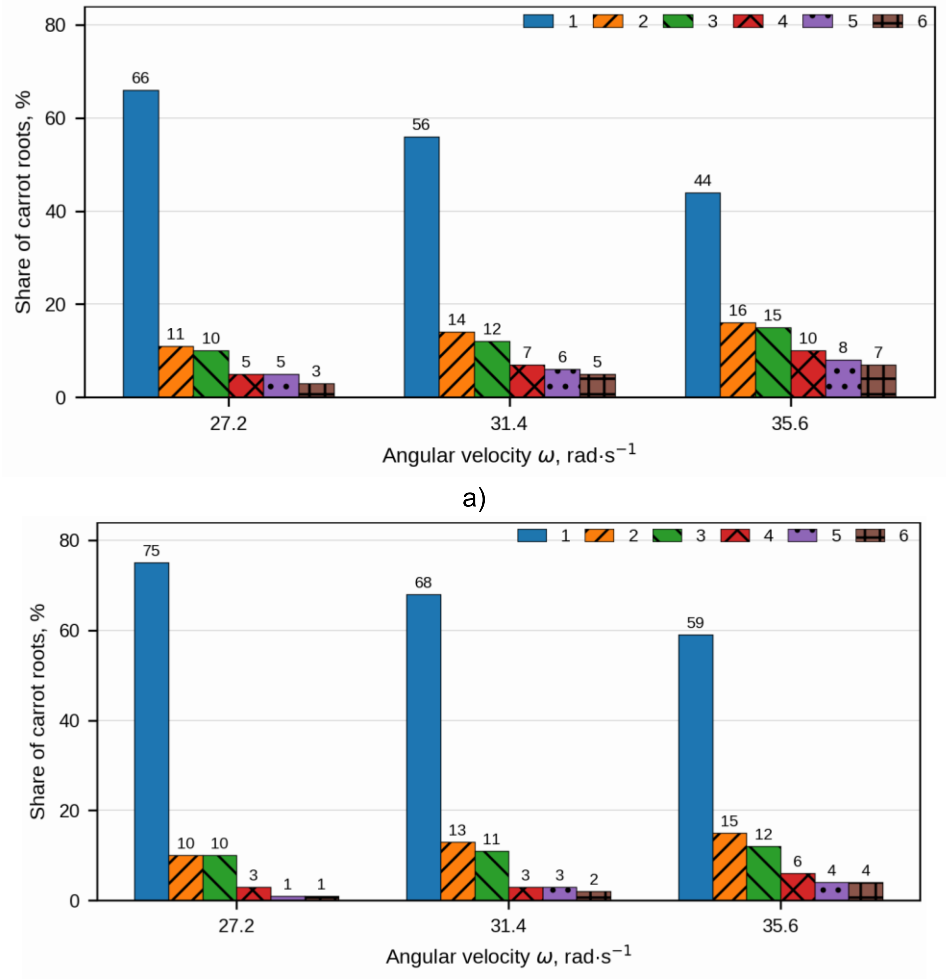

Fig. 5 – Distribution of damage categories at different angular velocities:
a – tail-end-first orientation; b – thicker-end-first orientation

1 – no damage; 2 – skin abrasions; 3 – scratches; 4 – cracks; 5 – broken tail end; 6 – impact bruise

DISCUSSION

Integrated assessment of operating modes. The two experimental components yielded a consistent mechanical interpretation. Thicker-end-first feeding resulted in a somewhat more even distribution of separated soil along the trough while reducing peak loading on the vulnerable tail end. The lowest damage level was obtained at ω = 27.2 rad·s^{-1} in the thicker-end-first orientation: 75% of roots had no visible defects, and the combined proportion of cracks, broken tail ends and impact bruises was 5%. However, the spatial distribution of separated soil is not equivalent to absolute cleaning efficiency because the available data did not include a complete balance of residual adhering soil for each operating mode. The identified mode should therefore be regarded as preferable according to the damage-minimization criterion, while final optimization for production conditions should consider a set of indicators: residual adhering soil, total separation, throughput, energy consumption and the proportion of mechanically damaged roots.

Comparison with published systems. A *Panax notoginseng* conveying-separating device achieved a separating rate of 93.60% and a screening rate of 92.64% under optimized bench conditions (*Wang et al., 2023*), while a self-propelled *Panax notoginseng* harvester reported a 96.8% net harvesting rate and 1.6% root damage (*Zhang et al., 2016*). Optimized potato separation systems reported 97.8% separation with 1.16% tuber damage (*Chen et al., 2024*) and 96% separation with 2% damage (*Pan et al., 2025*). A self-propelled white-radish combine reported 4.99% damage and 1.64% impurity (*Xiao et al., 2023*).

The 5% severe-damage proportion obtained here at 27.2 rad·s^{-1} with thicker-end-first feeding is close to the white-radish benchmark but higher than the 1.16-2% values reported for optimized Panax and potato systems. This comparison is indicative rather than direct: the cited studies evaluated whole harvesters or soil-crop complexes and used different damage thresholds, whereas the present protocol also counted superficial abrasions, scratches and bruises visible only after 24 h.

In addition, the present soil metric describes where separated soil was collected along the cleaner and is not an absolute separation efficiency or conveying rate. Consequently, the scientific contribution is the quantified effect of root orientation and angular velocity on the cleaning-damage trade-off.

In conclusion, it is particularly noteworthy that the movement of carrot roots within the cleaning channel of the newly developed soil-removal device differs substantially from that observed for other root crops. Furthermore, it's important to keep in mind that carrot roots themselves have specific shapes and sizes that are not comparable to those of potatoes, sugar beets, table beets, or fodder beets. This is particularly true for other root crops, such as *Panax notoginseng*, which cannot be effectively cleaned using the proposed device.

These two factors—the specific size and shape of carrot roots and the specialized design of the developed cleaner, which was specifically intended for cleaning carrot roots during harvesting—limit the relevance of direct comparisons with other root crops and cleaning devices. Consequently, the cleaning and damage results obtained in this study should not be directly compared with those reported for other root crops or cleaner designs. Moreover, the developed cleaner is unlikely to provide effective cleaning for root crops with substantially different morphological characteristics. The cleaning channel itself, consisting of spirals and a brush wall, was designed and manufactured solely for testing the cleaning of carrot roots from soil impurities using other types of cleaners and different types of root crops, is unlikely to be useful or relevant to scientists and designers.

Limitations and future work. The laboratory study used pre-dug Nantes roots, controlled entry orientation and a limited range of shaft speeds. Field-scale optimization should retain replicate-level tray masses and quantify residual adhering soil, total separation, throughput, energy consumption and random-orientation effects under varying soil moisture and root-size distributions. A future DEM-MBD model should be calibrated and validated against measured root trajectories, contact loads, zonal soil mass distributions and the observed damage categories; such a model was outside the scope of present experimental study.

CONCLUSIONS

1. An integrated method for evaluating the spiral cleaner was proposed, combining determination of the spatial distribution of separated soil in three cleaning-trough zones with two-stage inspection of mechanical damage to carrot roots.

2. Zone I accounted for 38-48% of the separated soil, Zone II for 33-41%, and Zone III for 11-28%. As angular velocity increased from 27.2 to 35.6 rad·s^{-1}, the Zone I share increased and the Zone III share decreased, indicating that intensive separation shifted towards the inlet of the trough.

3. The proportion of undamaged roots decreased from 66 to 44% in the tail-end-first orientation and from 75 to 59% in the thicker-end-first orientation. The latter orientation yielded 9-15 percentage points more undamaged roots and reduced the combined proportion of cracks, broken tail ends and impact bruises from 13-25% to 5-14%. Across all three angular-velocity strata, the common odds ratio for an undamaged root was 1.69 (95% CI 1.20-2.36; $p = 0.002$), while the odds of severe damage were reduced to 0.42 (95% CI 0.26-0.70; $p < 0.001$).

4. Under the tested conditions, $\omega = 27.2$ rad·s^{-1} in the thicker-end-first orientation was identified as the preferred operating mode according to the damage-minimization criterion. Establishing a global optimum will require a complete balance of residual adhering soil, together with measurements of throughput and energy consumption. Future work should also include field validation and development of a quantitatively validated DEM-MBD model.

REFERENCES

[1] Bulgakov V., Ivanovs S., Adamchuk V., Ihnatiev Y., (2017), Investigation of the influence of the parameters of the experimental spiral potato heap separator on the quality of work, *Agronomy Research*, vol. 15, no. 1, pp. 44-54.

[2] Bulgakov V., Nikolaenko S., Arak M., Holovach I., Ruzhylo Z., Olt J., (2018), Mathematical model of cleaning potatoes on surface of spiral separator, *Agronomy Research*, vol. 16, no. 4, pp. 1590-1606, DOI: 10.15159/AR.18.173.

[3] Chen M.D., Liu X.T., Hu P.X., Zhai X.T., Han Z.L., Shi Y.L., Zhu W.J., Wang D.W., He X.N., Shang S.Q., (2024), Study on rotor vibration potato-soil separation device for potato harvester using DEM-MBD coupling simulation, *Computers and Electronics in Agriculture*, vol. 218, article 108638, DOI: 10.1016/j.compag.2024.108638.

[4] Guo W., Campanella O.H., (2017), A relaxation model based on the application of fractional calculus for describing the viscoelastic behavior of potato tubers, *Transactions of the ASABE*, vol. 60, no. 1, pp. 259-264.

[5] Hevko R.B., Tkachenko I.G., Khomyk N.I., Gumeniuk Y.P., Flonts I.V., Gumeniuk O.O., (2020), Determination of technical-and-economic indices of root crop conveyer-separator during their motion on curved path, *INMATEH-Agricultural Engineering*, vol. 61, no. 2, pp. 175-182, DOI: 10.35633/inmateh-61-19.

[6] Hoffmann C., Engelhardt M., Gallmeier M., Gruber M., Märländer B., (2018), Importance of harvesting system and variety for storage losses of sugar beet, *Sugar Industry*, vol. 143, no. 8, pp. 474-484, DOI: 10.36961/si19782.

[7] Issa I.I.M., Zhang Z., El-Kolaly W., Yang X., Wang H., (2020), Design, ANSYS analysis and performance evaluation of potato digger harvester, *International Agricultural Engineering Journal*, vol. 29, no. 1, pp. 60-73.

[8] Jahanbakhshi A., Abbaspour-Gilandeh Y., Mesri Gundoshmian T., (2018), Determination of physical and mechanical properties of carrot in order to reduce waste during harvesting and post-harvesting, *Food Science & Nutrition*, vol. 6, no. 7, pp. 1898-1903, DOI: 10.1002/fsn3.760.

[9] Jin W., Xiang L., Peng G., Ming N., Qi W., Wen Z., (2020), Design and experiment of high-efficiency drag-reducing shovel for carrot combine harvester, *Transactions of the Chinese Society for Agricultural Machinery*, vol. 51, pp. 93-103 (in Chinese).

[10] Jin X., Du X., Wang S., Ji J., Dong X., Wang D., (2016), Design and experiment of stems cutting device for carrot harvester, *Transactions of the Chinese Society for Agricultural Machinery*, vol. 47, no. 3, pp. 82-89 (in Chinese).

[11] Nath S., Kumar A., Mani I., Singh J.K., Sureja A.K., (2019), Determination of physical and mechanical properties of carrot (Daucus carota) for designing combine harvesting mechanism, *The Indian Journal of Agricultural Sciences*, vol. 89, no. 6, pp. 1011-1016, DOI: 10.56093/ijas.v89i6.90825.

[12] Pan Y.F., Yang R.B., Zhang H., Zhang J., Zha X.T., Qiu Z.C., Wu M.S., (2025), Experiment and optimization of the potato-soil separation and conveying device for a harvester using RecurDyn-EDEM coupling simulation, *International Journal of Agricultural and Biological Engineering*, vol. 18, no. 4, pp. 149-156, DOI: 10.25165/j.ijabe.20251804.9219.

[13] Rybacki P., Przygodziński P., Osuch A., Osuch E., Kowalik I., (2024), Artificial neural network model for predicting carrot root yield loss in relation to mechanical heading, *Agriculture*, vol. 14, no. 10, article 1755, DOI: 10.3390/agriculture14101755.

[14] Stopa R., Komarnicki P., Szyjewicz D., Kuta Ł., (2017), Modeling of carrot root radial press process for different shapes of loading elements using the finite element method, *International Journal of Food Properties*, vol. 20, suppl. 1, pp. S340-S352, DOI: 10.1080/10942912.2017.1296862.

[15] Stopa R., Komarnicki P., Kuta Ł., Szyjewicz D., Słupska M., (2019), Modeling with the finite element method the influence of shaped elements of loading components on the surface pressure distribution of carrot roots, *Computers and Electronics in Agriculture*, vol. 167, article 105046, DOI: 10.1016/j.compag.2019.105046.

[16] Wang B., Hu Z., Gu F., Wu F., Cao M., Sun Y., (2025a), Analysis and evaluation of the experimental effect of double-disc knife-cutting device for carrot combine harvester, *Agriculture*, vol. 15, no. 7, article 682, DOI: 10.3390/agriculture15070682.

[17] Wang B., Hu Z., Wu F., Gu F., (2025b), Analysis and evaluation of harvest quality effectiveness of carrot clamping and conveying device, *Agriculture*, vol. 15, no. 3, article 275, DOI: 10.3390/agriculture15030275.

[18] Wang F.A., Wen B., Xie X.H., Jie K.T., Guo S.W., Zhang Z.G., (2023), Operation mechanism analysis and parameter optimization of conveying and separating device of Panax notoginseng harvester, *Transactions of the Chinese Society for Agricultural Machinery*, vol. 54, suppl. 1, pp. 201-211, 259 (in Chinese).

[19] Xia X., Xu Z., Yu C., Zhou Q., Chen J., (2021), Finite element analysis and experiment of the bruise behavior of carrot under impact loading, *Agriculture*, vol. 11, no. 6, article 471, DOI: 10.3390/agriculture11060471.

[20] Xiao X., Xie F.P., Zhao Z.Q., Liu D.W., Wang X.S., (2023), Design and experimentation of a self-propelled picking type white radish combine harvester, *Agriculture*, vol. 13, no. 8, article 1578, DOI: 10.3390/agriculture13081578.

[21] Yasmeen Z., Ashraf M., Ahmad S., Ahmad M., Sabir I., Shahzaib, (2023), Development and economic evaluation of carrot harvester cum trimmer, *Journal of Agricultural Research*, vol. 61, no. 1, pp. 65-76, DOI: 10.58475/2023.61.1.1837.

[22] Zeng G.J., Chen J.N., Xia X.D., (2018), Design and experiment on pull type of tassel-fruit separation for carrot, *Transactions of the Chinese Society for Agricultural Machinery*, vol. 49, pp. 73-79 (in Chinese).

[23] Zhang Z.G., Wang F., Zhang Y.C., Zhang D., Tian R., (2016), Design and experiment of self-propelled Panax notoginseng harvester, *Transactions of the Chinese Society for Agricultural Machinery*, vol. 47, suppl. 1, pp. 234-240 (in Chinese).

[24] Zhao Z.H., Wang J.S., Yang L.L., Shao Z.T., (2024), Optimal design of carrot digging shovel based on discrete element method, *Journal of Agricultural Mechanization Research*, vol. 46, pp. 139-145 (in Chinese).

[25] Zhou W., Song C., Song K., Wen N., Sun X., Gao P., (2023), Surface defect detection system for carrot combine harvest based on multi-stage knowledge distillation, *Foods*, vol. 12, no. 4, article 793, DOI: 10.3390/foods12040793.